Studies of Free-Boundary Field-reversed Configurations with Improved Stability in the Magnetic Reconnection Experiment

S.P. Gerhardt 1), M. Inomoto 2), E. V. Belova 1), M. Yamada 1), H. Ji 1), Y. Ren 1)
1) Princeton Plasma Physics Laboratory, Princeton, NJ, USA
2) Osaka University, Osaka, Japan
e-mail contact of main author: sgerhard@pppl.gov

Abstract. The stability of oblate FRCs formed by counter-helicity spheromak merging is studied in the Magnetic Reconnection Experiment (MRX). Stability to n=1 tilt/shift modes is improved by either plasma shaping or installation of a passive stabilizer. Newly identified n≥2 co-interchange modes often then limit the plasma lifetime, and can be reduced by forming very oblate plasmas. Equilibrium studies confirm the external control of the plasma shape. The stability improvement in very oblate plasmas is consistent with predictions by a rigid-body model and MHD computation.

1. Introduction

The field-reversed configuration (FRC) [1] is a unique configuration for magnetic fusion energy: the configuration has a toroidal plasma current, but no toroidal magnetic field. This leads to a number of advantages as the core of a fusion system: a simply connected geometry, beta of order unity, a natural divertor structure, and a possible separation of the formation and fusion burn regions. However, the intrinsically bad curvature of the field lines in an FRC leads to a host of magnetohydro-dynamic (MHD) instabilities [1]. The most feared instability in the traditional prolate (axially-elongated) FRC is the internal tilt. This instability is predicted to grow on the Alfven transit time and is difficult to stabilize with nearby conductors because the tilt motion is internal to the separatrix. Interestingly, this instability has never been conclusively observed in a prolate FRC. The most likely region for the surprising stability is stabilization due to finite-Larmour radius (FLR) effects [2,3]; nearly all prolate FRCs to date have been produced in the regime where kinetic effects should be important.

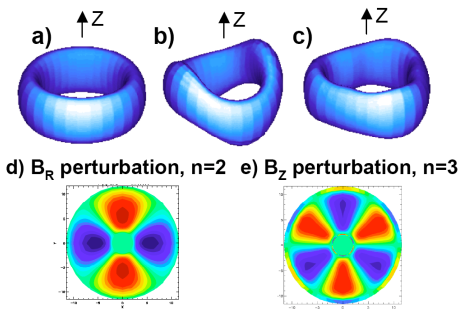

FIG. 1. a) Unperturbed pressure isosurface, isosurface after b) an axially polarized n=2 mode, and c) a radially polarized n=3 mode. Also shown are d) the midplane B_R perturbation for the axially polarized n=2 mode and e) the midplane B_Z perturbation for the radially polarized n=3 mode.

The concern about the stability of the prolate FRC in the reactor-relevant MHD regime has motivated recent experimental [4,5] and theoretical [6] study of oblate FRCs, where the plasma boundary is more spherical in shape. The tilt mode in these configurations is an external mode, and can be completely stabilized in a sufficiently oblate plasma [6,7], although a radial shifting mode then becomes unstable [6,7]. Both of these n=1 modes can be stabilized by near-fitting conducting structures [6] (n is the toroidal mode number). Furthermore, the spherical shape maximizes the shortest distance between the hot plasma core and the cool plasma edge. However, even with nearby conductors, these plasma are unstable to co-interchange modes [8,9,10], which are the n≥2 cousins of the tilt and shift modes. These modes have the displacement localized in the region of maximum curvature (ballooning-like). An example of an n=2 axially polarized co-interchange is given in Fig. 1b; the dominant fluid displacement is in the axial (z) direction. A radially polarized n=3 co-interchange is illustrated in Fig. 1c; the dominant fluid displacement is in the radial direction. These computations were done with the

HYM code [11], which predicts that both polarizations and many mode numbers can be simultaneously unstable. Although these modes grow until the configuration is destroyed in simulation, they have never previously been identified in an experiment.

The FRC research in the Magnetic Reconnection Experiment (MRX) [12] has commenced with the study of oblate FRC stability [13], both with and without a central stabilizing column. The deadly external tilt can be mitigated by i) utilizing a conducting center-column over a range of elongations, or ii) forming very oblate plasmas in which case the center-column is not necessary. The n≥2 axially polarized co-interchange modes are often unstable, even in the presence of the passive stabilizer, and often grow until the equilibrium is lost. Forming plasmas with a very oblate shape results in the minimum amplitude of these modes, and the longest plasma lifetime. Equilibrium analysis has demonstrated the control of the FRC shape through the external magnetic field configuration, and stability analysis has confirmed that the oblate shape of FRCs in MRX leads to improved stability.

2. Description of Experiments

Oblate FRCs are formed in MRX via the merging of two spheromaks with oppositely directed toroidal fields [14]. The two spheromaks are formed with flux-cores at opposite end of the device; the toroidal windings ("PF" coils) of the flux cores provide a portion of the equilibrium vertical field after merging is completed. The large "EF" coils and the shaping field ("SF") coils provide further equilibrium field; the equilibrium field shape can be changed by adjusting the currents in these various coils. The SF coils were centred at Z=±0.15 m and the PF coils at Z=±0.55 for these experiments. We use the equilibrium field mirror ratio

$$MR = \frac{B_Z(R = 0m, Z = 0.55m)}{B_Z(R = 0m, Z = 0m)}$$

to parameterize the field spatial structure.

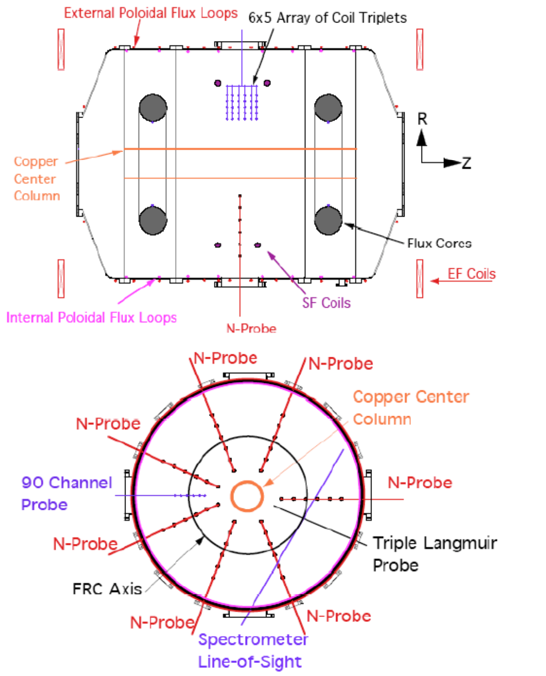

FIG. 2. (top) Side-view of MRX showing flux-cores, SF & EF coils, center-column, and the 90-channel probe array. (bottom) End-on view of MRX illustrating the N-probe array.

A variety of optical and probe diagnostics are used to diagnose the plasma. The "90-channel" probe is a 6x5 array of coil triplets, measuring all components of the magnetic field with 4 cm spatial resolution in the R-Z plane. The "N-probes" are an array of 7 probes inserted at the midplane (Z=0), each with 5 coil triplets spaced by 8 cm. This array allows measurement of the midplane magnetic perturbation with toroidal mode number up to n=3, in all components of the magnetic field. The plasma density and electron temperature are measured with a triple Langmuir probe, and the ion temperature is measured via the Doppler broadening of the HeII spectral line at 468.6 nm.

In order to study the effects of passive stabilization on the FRC plasma, a copper center-column was installed in the center of the device for some discharges [6]. It has a 10cm radius, with a thickness of 0.63 cm. There is an axial cut to prevent toroidal currents from flowing, in order to not interfere with spheromak formation and the plasma equilibrium.

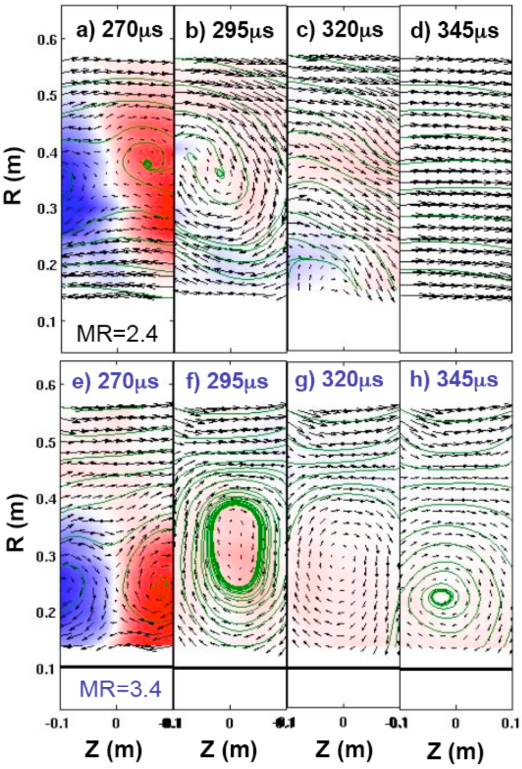

FIG. 3. (a-d) Four images of the time evolution of a discharge which develops a large n=1 tilt mode (no center-column, MR=2.4), and (e-h) four similar images from a very oblate plasma with a center-column (MR=3.4), which displays more robust stability. Some streamlines (green, not flux lines) are illustrated to guide the eye. Colors represent toroidal fields from -0.5 to 0.5 Tesla, with red positive.

3. Experimental results regarding oblate FRC stability.

We have used the measured midplane magnetic perturbations to diagnose the instabilities observed in MRX [13]. This diagnosis is informed by the computed magnetic perturbations from HYM. These calculations indicate that axially polarized instabilities (Fig. 1b) tend generate a large B_R perturbation at the midplane, as illustrated in Fig.1d, when the poloidal field of the FRC is dragged into the midplane. Radially polarized instabilities (Fig. 1c) tend to generate large B_z perturbations, as illustrated in Fig. 1e. Hence, the B_R perturbation will be interpreted as indicative of axially polarized modes, and the B_Z perturbation as indicative of radially polarized modes.

Helium FRCs have been formed in MRX over a large range of external field mirror ratio, both with and without a center-column, demonstrating a variety of stability behaviors. A series of "snap-shots" from two configurations is illustrated in Fig. 3; this data was compiled by between-shot scanning of the 90-channel probe through three locations and averaging the resulting discharges. The discharge in (a-d) is for a low mirror ratio case without a center-column. The plasma in this case is quickly terminated by an instability (shown below to be the n=1 tilt). The plasma in Fig. 3 (e-h) is a high mirror ratio case with the center-column present; the plasma lasts significantly longer, and the decay is largely axisymmetric.

Fig. 4 illustrates a) the poloidal flux at the field null (ψ_{null}), b) the B_R, n=1 amplitude, and c) the B_R, n=2 amplitude as a function of time for three different sets of discharges. The grey area indicates the time before merging is complete. The black curves correspond to the MR=2.4 case with no center-column, illustrated in Fig. 3(a-d). The poloidal flux shows poor reproducibility in this case, due to the large B_R, n=1 (tilt) mode which grows even before merging is finished. This tilt leads to the immediate termination of the plasma. The red curves correspond to a MR=2.4 case, but with the center-column present. Although the n=1 tilt is eliminated by the stabilizer, a B_R, n=2 mode grows immediately after merging is finished. This n=2 axially polarized co-interchange mode leads to the quick destruction of the

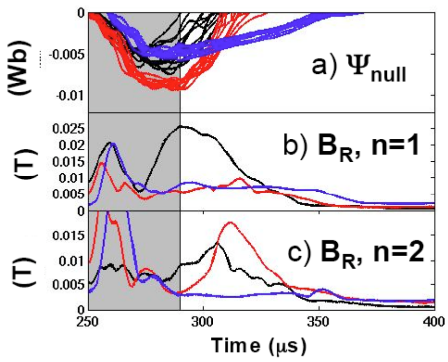

FIG. 4. Time evolution of (a) the poloidal flux at the field null, (b) the B_R, n=1 perturbation, and (c) the B_R, n=2 perturbation.

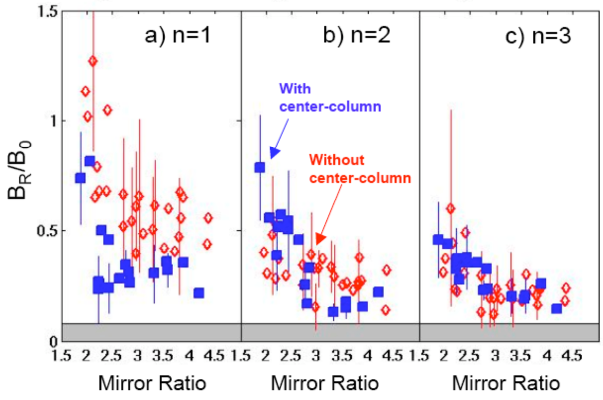

FIG. 5. Amplitude of the B_R perturbations: a) n=1, b) n=2, & c) n=3, as a function of external field Mirror ratio. Red, open (blue, closed) symbols correspond to discharges without (with) the center-column.

configuration. Finally, the blue curves illustrate the evolution of a configuration with a large mirror ratio (MR=3.4) and the stabilizer, as illustrated in Fig. 3 (e-h). No large instabilities grow, and the plasma decays on a much longer time-scale. Note that large non-axisymmetries are present during the merging process in a three examples; in some cases, the magnetic perturbations grow, and in others, they stay constant or are reduced in time.

These trends are illustrated more systematically in Fig. 5, where the B_R perturbation amplitudes are shown as a function of mirror ratio. The amplitude shown is the largest amplitude after merging is completed, and have been normalized to the B_Z field at the separatrix immediately after merging; the error-bars represent shot-to-shot variability. Discharges without a center-column (red, open) show a large n=1 amplitude, corresponding to the tilt mode. The amplitude of the tilt decreases as the mirror ratio is increased, as expected when the plasma becomes more oblate [6,7]. The n=1 signature is drastically reduced by the center-column (blue, closed), except at very low mirror ratio. The n=2&3 mode amplitudes are not strongly effected by the presence of the center-column. We have observed that the n=1 perturbation is more broad than the n=2&3 perturbations [13], allowing it to interact more easily with the center-column; this decrease in the effectiveness of passive stabilization for higher-n modes is consistent with predictions from HYM calculations [6]. These n=2&3 mode amplitudes are observed to decrease with increasing mirror ratio.

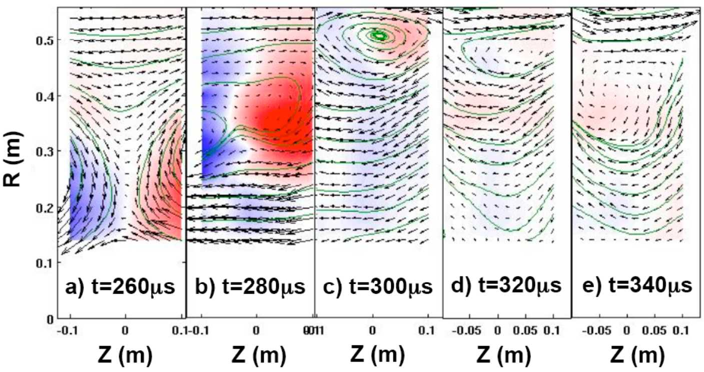

FIG. 6. Shifting motion for a large mirror ratio discharge without the center-column. The plasma shifts outward and back at the angle of the 90-channel probe, on a time-scale shorter than the discharge lifetime.

The n=1 perturbation to B_Z (not shown), indicative of the radial shifting mode, shows an increasing amplitude as the mirror ratio is increased in the absence of the center-column [13]. This is in keeping with the prediction [6,7] that the radial shifting mode should become unstable for very oblate plasmas. We have observed, however, that the radial shift tends to saturate in the present geometry, as illustrated in Fig. 6 for a high mirror ratio case without the center-column. The plasma shifts out at the toroidal angle of the 90-channel probe (which was used to take these “snap shots”), but then reflects back to a more centered location; the shift and “reflection” occur on a time shorter than the plasma lifetime. The “reflection” is most likely due to the strong magnetic field at large radii between the shaping coils. The radial shifting mode is largely suppressed by the center-column. The n=2 & 3 B_z perturbations, indicative of the radially polarized co-interchange, do not show a strong dependence on the mirror ratio or the presence of the center-column.

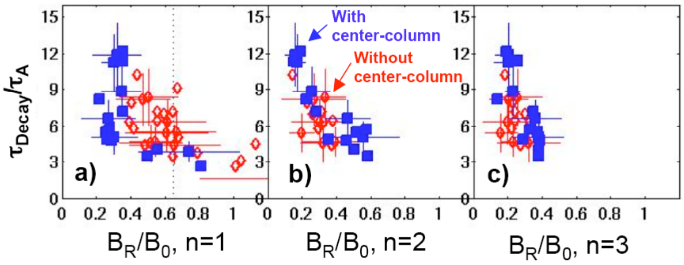

FIG. 7, Dependence of the plasma decay-time on the normalized B_R perturbations. The points on the right of the dotted line in (a) are not plotted in (b) and (c). Red, open (blue, closed) symbols correspond to discharges without (with) the center-column.

We have determined that the axially polarized co-interchange modes, indicated by a B_R perturbation, are the most dangerous modes for the present FRCs in MRX. The lifetime of the FRC is approximate by the 1/e time of the decay of the field reversal, and is plotted as a function of the maximum B_R perturbation amplitude in Fig. 7. The time are normalized to the Alfven time. Considering Fig. 7a, it is clear that when the B_R, n=1 (tilt) amplitude is large, the plasma does not last for longer than a few Alfven times. Reducing the n=1 amplitude can be accomplished by introducing a center-column (closed symbols), or by forming plasmas with large mirror ratios (and hence the smallest tilt-perturbation amplitude, see Fig.5). Note that for low n=1 amplitude, there is still significant scatter in the lifetime. The data is re-plotted in Fig. 7(b) & (c) as a function of the B_R, n=2&3 amplitudes, where all points with large n=1 amplitude (right of the dashed line in Fig. 7a) have been removed. There is a clear trend of decreasing lifetime with increasing n=2&3 amplitudes. This data strongly indicates that the elimination of the n=1 (tilt) mode is not sufficient for the formation of long-lived FRCs. The n=2&3 axially polarized co-interchange modes can grow until the configuration is terminated.

We do not observe any correlation between the B_Z perturbations and the lifetime of the plasma [13]. This is due to the finite growth of the shift-like modes, as discussed in relation to Fig. 6.

4. FRC Equilibrium and Stability Calculations

We have conducted FRC equilibrium studies [13] by solving the Grad-Shafranov (GS) equation, subject to the measured magnetic field information. The MRXFIT code uses an iterative technique [15] to solve the GS equation. The magnetic fields and poloidal flux from the plasma currents and coils internal to the vacuum vessel (SF and PF coils) are computed using Green's functions that automatically incorporate the flux-conserving nature of the vacuum vessel. The result of the GS solution includes the toroidal plasma current distribution, the poloidal flux, the pressure profile, the poloidal current distribution, and the magnetic field at the locations of selected diagnostics.

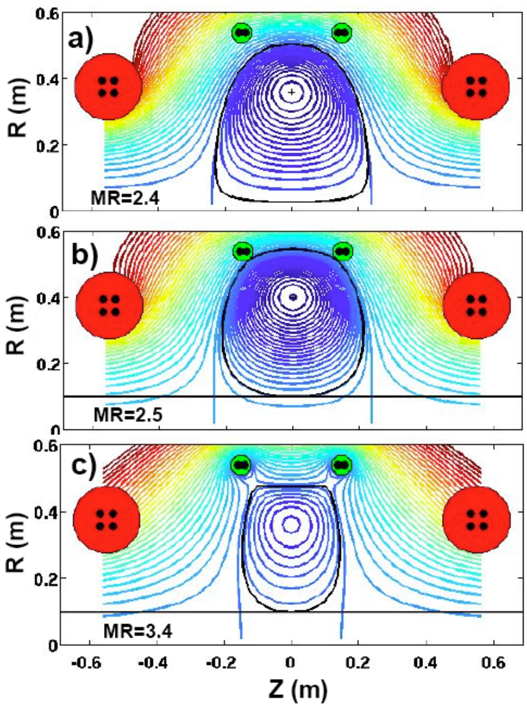

FIG. 8. Poloidal flux contours from example equilibria for three different FRCs in MRX.

The fitting procedure begins when the pressure profile p(ψ) and F(ψ)F'(ψ), where $F=RB_T/\mu_0$, are fit to an analytic solution of the GS equation [16]. The analytic solution is then mapped to a simple polynomial in ψ, and the GS equation is solved using the iterative technique. This solution is used to predict the diagnostic signals, which are compared to measurements. The pressure profile and poloidal current distribution are then varied until a good match is found between the calculation and the data. We use the n=0 components of the N-probe B_Z and B_T data as a constraint on the equilibrium; the data from the 90-channel probe (single toroidal angle), is not necessarily a good indicator of the axisymmetric equilibrium.

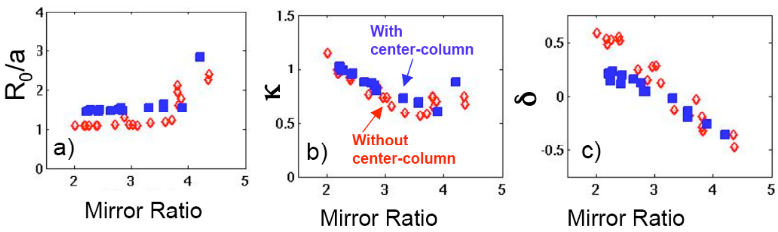

FIG. 9. The aspect ratio (a), elongation (b), and triangularity (c) as a function of Mirror Ratio. Open symbols correspond to discharges without a center-column, and closed symbols for discharges with a center-column.

Three example FRC equilibria are illustrated in Fig. 8. These three equilibria are for the cases described in Fig. 4. The example in Fig. 8a) has no center-column and a lower mirror ratio (MR=2.4). This plasma shows the standard X-points of an FRC equilibria and extends to the geometric axis of the device. Note, however, that due to the rapid growth of the tilt in this case, this equilibrium calculation can only be treated as an approximation to the actual configuration. The plasma in Fig. 8 b) has a similar mirror ratio at the previous case, but is instead limited by the center-column. The third calculation illustrates the effect of having a large mirror ratio, which is achieved by having the current in the shaping coils (green in figure) parallel to the plasma current, and opposed to the current in the PF coils (red) and EF coils (not shown). X-points form between the shaping coils and the plasma boundary, and for sufficiently high mirror ratio, these X-points define the plasma boundary. Note the region of strong field and good curvature between the shaping coils and at large radii, which likely leads to the saturation of the n=1 radial shift.

The shaping field coils can be used to systematically vary the shape, and hence stability, of the plasma. This is illustrated in Fig. 9, where the shape parameters are plotted as a function of mirror ratio. The parameters are defined as $a = (R_o - R_i)/2$, $R_0 = (R_o + R_i)/2$, $\kappa = Z_t/a$, $\delta = (R_0 - R_t)/a$ [16]. These definitions use R_i and R_o as the inner and out radial coordinates of the plasma boundary at Z=0 and R_t and Z_t as the point on the boundary with the maximum value of Z. Note that this definition of elongation (κ) is twice the value typically used in FRC research. The aspect ratio of the plasma increases at large mirror ratio, mainly due to a decrease in the minor radius. Note that the plasmas without the center-column typically have a lower aspect ratio, since the center-column generally acts as a limiter when it is present. The elongation (κ) and triangularity (δ) generally decreases as the mirror ratio is increased. These configurations unique δ<0 tend to have the optimum performance.

We have used a rigid-body model [7] to understand the n=1 tilt/shift stability of MRX plasmas. The model is based on treating the plasma as a series of current rings, which shift or tilt in unison in response to the force from the external coils. The torque resulting from a small tilt θ_X is given by

$$N = \theta_X \sum_i \pi R^2 \left| I_i B_{Z,i} \right| \left(1 - n_{decay,i} \right) \tag{1}$$

where $n_{decay} = -\frac{R}{B_Z}\left[\frac{\partial B_Z}{\partial R} - \frac{Z}{R^2}\frac{\partial}{\partial R}\left(2RB_R + ZB_Z\right)\right]$, all field quantities correspond to those from external magnets only (including image currents induced in the vacuum vessel wall), and the sum is over the current rings. If this torque is positive, the small tilt will be reinforced and the tilt instability will grow. The force on the current rings after a small radial displacement ξ is given by $F = -\xi\pi\sum_i \frac{\partial B_Z}{\partial R} R_i I_i$. If this force is positive, the radial shift instability will grow. Note that the rigid-body model fails to fully account for the stabilizing impact of the center-column, does not include stabilizing effects such as line-tying, and does not model the true tilt/shift eigenfunctions; we utilize it here to gain some physical intuition while acknowledging these limitations. The MRXFIT equilibria are used in the application of this model.

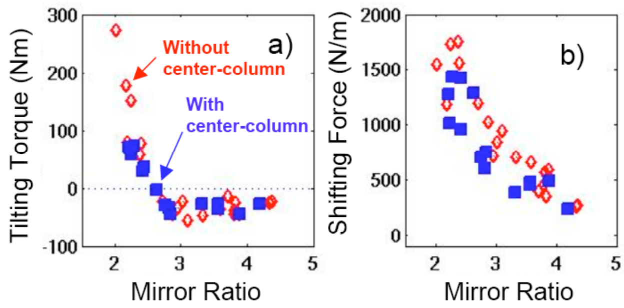

FIG. 10. Tilting torque and shifting force, normalized to the small tilt and displacement, respectively, as a function of the mirror ratio.

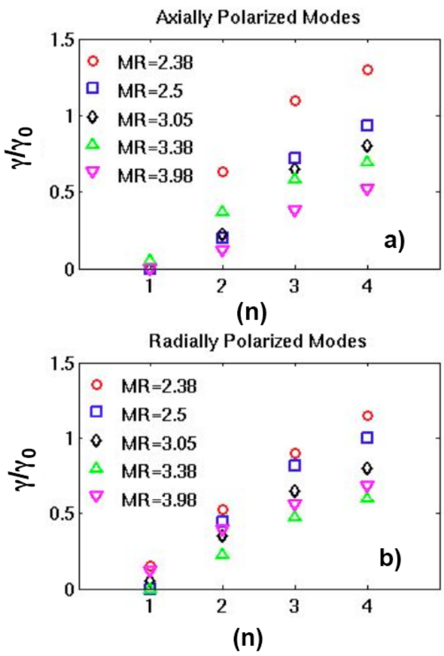

FIG. 11. Linear Growth rates of low-n co-interchange modes (axial and radial polarizations) for FRCs with different mirror ratios.

The torque and force have been computed as a function of mirror ratio, and are displayed in Fig. 10. A small correction was made for the effects of n=1 eddy currents in the center-column. The calculations predict that the plasma will transition from a tilt-unstable to a tilt-stable regime when the mirror ratio exceeds ~2.5. This is similar to the experimental boundary observed for the elimination of the destructive tilt. Note that large n=1 perturbations, often remaining from the formation phase, are observed for plasmas with MR>2.5, but the n=1 mode is typically not the cause of the ultimate termination of the discharge. The shifting force is always positive for these equilibria, implying that the plasma should be unstable to a radial shifting mode. In the absence of the center-column, we do indeed observe a radial shifting motion, as indicated in Fig. 6. The plasma is observed to "bounce off" the region of high magnetic field strength, an effect not captured by the rigid-body model.

We have conducted linear and non-linear stability calculations of these FRCs using the HYM code [11], based on the MRXFIT equilibria. The linear stability calculations include the full plasma shaping and the effects of the center-column. The linear growth rates for axially and radially polarized co-interchanges modes are shown, for five different configurations, in Fig. 11. The growth rate of the modes increases with the mode number, as expected in MHD. No absolute stability is found, as anticipated for an MHD system with bad curvature everywhere [10]. However, for fixed toroidal mode-number, the growth rate is reduced by increasing the mirror ratio, a trend consistent with the experimental results. Note that both axially and radially polarized instabilities are reduced as the mirror ratio is increased, implying the unique favorable features of these highly oblate configurations. Non-linear calculations (without the center-column) have indicated that the outward motion of radially polarized co-interchange modes is stabilized by the large field strength on the outboard side of the device [13].

We estimate that these Helium plasmas are in the MHD regime for the low-n instabilities discussed in this paper. The condition for finite-Larmour radius stabilization is $\gamma<\omega^*$, where γ is the MHD growth rate determined from calculations such as in Fig. 11, and $\omega^* = kv_D = \frac{Tk}{eBL_P}$ is the diamagnetic frequency [6] (with L_P the pressure scale length). Applying this condition to the MRX plasmas leads to the conclusion that FLR effects begin to play a role for n>3-4. We note that these higher-n modes may not lead to disruption, but rather to enhanced heat, particle and flux loss from the system.

5. Summary

We have studied the stability properties of oblate FRCs formed by counter-helicity spheromak merging [13]. The destructive n=1 tilt instability has been eliminated by i) forming very oblate plasmas, or ii) stabilizing the plasma with a copper center-column. The n=1 radial shift mode is eliminated by the center-column, and is observed to saturate in the case without a center-column. Co-interchange modes with n≥2 have been observed, and can limit the plasma lifetime; these mode amplitudes can be reduced, and the plasma lifetime extended, by forming very oblate plasmas with triangularity $\delta<1$. A rigid-body stability calculation has shown that these very oblate plasmas are indeed in a regime which is stable to the n=1 tilt mode, and HYM calculations indicate a reduction in the linear growth-rate of co-interchange modes for these very oblate plasmas.

The authors acknowledge the advice and assistance of R. Cutler, D. Cylinder, and A. Kuritsyn. This research was funded by the United States Department of Energy.

References:

[1] TUSZEWSKI, M., *et al.*, Nuclear Fusion **28**, (1988) 2033.
[2] BELOVA, E.V., *et al.*, Phys. Plasmas **13**, (2003) 2361
[3] TUSZEWSKI, M., *et al.*, Phys. Fluids B **3**, (1991) 2856
[4] KAWAMORI, E., *et al.*, Phys. Rev. Lett **95**, (2005) 085003
[5] COTHRAN, C.D., *et al.*, Phys. Plasmas **10**, (2003) 1748
[6] BELOVA, E.V., *et al.*, Phys. Plasmas **8**, (2001) 1267.
[7] JI, H., *et al.*, Phys. Plasmas **5**, (1998) 3685.
[8] NEWCOMB, W.A., *et al.*, Phys. Fluids **23**, (1980) 2296.
[9] ISHIDA, A., *et al.*, Phys. Plasmas **1**, (1994) 4022.
[10] CARY, J.R., Phys. Fluids **24**, (1981) 2239.
[11] BELOVA, E.V., *et al.*, Phys. Plasmas **7**, (2000) 4996.
[12] YAMADA, M., *et al.*, Phys. Plasmas **4**, (1997) 1936.
[13] GERHARDT, S.P., *et al.*, accepted for publication in Phys. Plasmas.
[14] YAMADA, M., *et al.*, Phys. Rev. Lett. **65**, (1990) 721.
[15] ANDERSON, J, K., *et al.*, Nuclear Fusion **44**, (2004) 162.
[16] ZHENG, S.B., *et al.*, Phys. Plasmas **3**, (1996) 1176.